Tellus (2007), 59A, 618–626
Printed in Singapore. All rights reserved

© 2007 The Authors
Journal compilation © 2007 Blackwell Munksgaard

TELLUS

Thermal decay modes of a 2-D energy balance climate model

By WEI WU [1,2]* and GERALD R. NORTH[1], [1]*Department of Atmospheric Sciences, Texas A&M University, College Station, Texas 77843-3150, USA;* [2]*Department of Atmospheric Sciences, University of North Dakota, Grand Forks, North Dakota 58202-9006, USA*

(Manuscript received 31 July 2006; in final form 23 February 2007)

ABSTRACT

A complete series of non-orthogonal thermal decay modes (TDMs) of climate is derived from a two-dimensional (2-D) Energy Balance Climate Model (EBCM) and their properties are investigated. The orthogonality property is broken by the presence of the land–sea distribution through the effective heat capacity function. In the model, these mode amplitudes decay exponentially when the same component of forcing is made to vanish. If the projection of forcing is white noise in time, the mode amplitudes will have Lorentz spectral densities (i.e. first order Markov or first-order Autoregressive Process (ARI)) making the autocorrelation functions decay exponentially as well. The TDM have family-style shapes: all oceans, Eurasian–African family, North American family, etc. When actual data are projected onto the mode patterns their time-series exhibit the same exponential decay behaviour. These modes are proven useful in studying the global surface temperature field. The development of the TDM theory makes it possible to analyse more generally time-dependent surface-temperature problems in a framework with physical interpretation.

1. Introduction

Energy conservation constrains the earth's surface temperature to be determined by a balance of the rate of incoming solar energy absorbed by the Earth and the rate of outgoing energy by infrared radiation and other non-radiative processes. Energy Balance Climate Models (EBCMs) are simple climate models whose solutions yield the surface temperature field and its variability as reviewed by North et al. (1981). A fundamental assumption in setting up the model is that the parameters are piecewise constant, taking a single value over land and a different one over ocean. The major advantage of these models is that they have only a few adjustable parameters and therefore solutions can be easily extracted by either analytical or reliable numerical procedures. The disadvantage of these models is that they do not have an explicit advection term and some non-radiative heat flux terms such as latent and sensible heat fluxes are highly simplified through a simple diffusive parametrization. The fundamental principle of such climate models is the conservation of energy for each infinitesimal horizontal cross-section of Earth–Atmosphere column.

EBCMs account for the energy fluxes into and out of the Earth–Atmosphere column. All the fluxes are parametrized in terms of the surface temperature field (North et al., 1981). Horizontal heat transports are parametrized by simple diffusive mechanisms and the infrared radiation to space by an empirical linear form in surface temperature. EBCMs have proven to be useful models for examining idealized climate systems and for exploring questions not easily handled with large models, such as GCMs (North et al., 1981). They have been successful in modelling climate and climate change of the surface temperature field and have been making great contributions to climate studies for three decades. The phenomenological parameters, such as diffusion or radiative damping coefficients in EBCMs cannot be derived directly but rather have to be fitted to real data (North et al., 1981). A few such adjustable parameters are required to obtain good fits to the geographical distribution of such quantities as the mean seasonal cycle and the distribution of variance over a wide range of frequency bands. The time scale separation of the eddies that transport most of the heat (days), and the radiative relaxation time of a column of air (weeks) or the relaxation time of the mixed layer of the ocean (months) lead to the success of the models in reproducing the observed fields.

Because of their simplicity, the models have been playing an important role in testing and predicting global climate change (e.g. Frame et al., 2005; Hegerl et al., 2006). However, some aspects of the spectral behaviours of the surface temperature in EBCMs have not been explored. In this paper, we will introduce a complete set of time independent thermal decay modes (TDM) from the EBCM as introduced by North et al. (1983; hereafter,

* Corresponding author.
e-mail: wwu@aero.und.edu
DOI: 10.1111/j.1600-0870.2007.00245.x

NMS83) in an effort to bring a better understanding for the spectral behaviours of the Earth surface temperature in the EBCM. These modes can serve as a basis set for studying the global surface temperature field.

2. Deriving the thermal decay modes

The EBCM of NMS83 is written as

$$C(\hat{r})\frac{\partial T(\hat{r},t)}{\partial t} - \nabla\cdot(D(\hat{r})\nabla T(\hat{r},t)) + A + BT(\hat{r},t) = F(\hat{r},t), \tag{1}$$

where $T(\hat{r},t)$ is the surface temperature field at point $\hat{r}$ and time t, $C(\hat{r})$ is the heat capacity field which is large over ocean (the value estimated from the mixed layer depth) and roughly two orders of magnitude smaller over land (characteristic of a fraction of the atmosphere/land portion of the column, usually fitted from seasonal data), $D(\hat{r})$ is a thermal conductivity coefficient which might depend upon position on the sphere, $A + BT$ is the rate of outgoing infrared radiation to space with A and B empirical coefficients derived from satellite measurements (e.g. Graves et al., 1993).

$F(\hat{r},t)$ is an external forcing which could include the mean annual $QS_{m.a.}(\mu)(1-\alpha(\hat{r}))$, with Q the solar constant $\div 4$ ($\approx$340 W m^{-2}); $S_{m.a.}(\mu) = 1 - 0.477P_2(\mu)$ the mean annual distribution of solar radiation energy reaching the top of the atmosphere at sine of latitude μ; $P_n(\mu)$ is the $n-$th Legendre Polynomial, and the second Legendre Polynomial $P_2(\mu) = \frac{1}{2}(3\mu^2 - 1)$; $\alpha(\hat{r})$is local albedo). If one wants to look at the seasonal cycle, $S(\mu, t)$ contains seasonal terms (given in the next section). A noise forcing representing weather fluctuations can also be added to the right-hand side as a part of $F(\hat{r},t)$ (e.g. Stevens and North, 1996). In the present analysis, the cloud forcing from the infrared radiation is assumed to exactly cancel the cloud forcing due to the solar radiation.

The equation for the temperature departure (remove the annual-mean part) formed by (1) is

$$C(\hat{r})\frac{\partial \tilde{T}(\hat{r},t)}{\partial t} - \nabla\cdot(D(\hat{r})\nabla \tilde{T}(\hat{r},t)) + B\tilde{T}(\hat{r},t) = \tilde{F}(\hat{r},t). \tag{2}$$

$\tilde{F}(\hat{r},t)$ represents periodic and/or noise forcing. If $\tilde{F}(\hat{r},t)$ is assumed to be zero, we can analytically solve the linear eq. (2) by setting $\tilde{T}(\hat{r},t) = \psi(\hat{r})e^{-\lambda t}$. This leads to a generalized Sturm–Liouville eigenvalue problem as follows

$$(-\nabla\cdot D(\hat{r})\nabla + B)\psi(\hat{r}) = \lambda C(\hat{r})\psi(\hat{r}). \tag{3}$$

The LHS operator $-\nabla\cdot D(\hat{r})\nabla + B$ is Hermitian (Horn and Johnson, 1985; see also Appendix for a short review of pertinent mathematical definitions). Boundary conditions are no heat flux entering the poles. The result is a complete basis set of eigenfunctions $\psi_n(\hat{r})$ (referred to here as the thermal decay modes) corresponding to eigenvalues λ_n (n = 1, 2, 3, ...). These eigenvalues and eigenfunctions are real (Horn and Johnson, 1985). Note that $\frac{C(\hat{r})}{B}$ has dimension time and is the characteristic time for relaxation at the point $\hat{r}$ (e.g. North and Coakley, 1979). The quantity $\frac{D(\hat{r})}{B}$ is the square of a local diffusive length scale (e.g. Lindzen and Farrel, 1977).

The system (3) is 2-D on the surface of the sphere and it has the position-dependent factor $C(\hat{r}) \geq 0$ on the RHS multiplying the eigenvalue, λ_n, with n running over the positive integers from one to infinity. We will order the eigenfunctions and eigenvalues such that the smallest values of n correspond to the largest time scales ($\tau_n = \lambda_n^{-1}$). As we will see these longest time scales will be associated with the modes identifiable as large-scale ocean features. These will have characteristic times of the order of 1 yr according to our inclusion of only the mixed layer of the ocean. It is implicit that certain boundary conditions, such as finiteness at the poles are part of the expression of the eigenvalue problem. In (3), we have anticipated that the eigenvalues, λ_n, and eigenfunctions, $\psi_n(\hat{r})$, will form a discrete set labelled by the integer index n. The eigenvalues and eigenfunctions of such a system are real (or can be chosen to be so by suitable linear combinations) and that the eigenfunctions are not necessarily orthogonal (see the Appendix). However, it is possible to show that a weight function (the heat capacity function $C(\hat{r})$) can be introduced to facilitate expansions in these functions (the TDMs) as follows:

$$(\psi_m, C\psi_n) = \delta_{m,n}. \tag{4}$$

The standard inner product notation is introduced in Appendix (16). A special case arises when $C(\hat{r})$ and $D(\hat{r})$ are both constant over the globe. In that case the eigenfunctions are just the spherical harmonics $Y_{n,m}(\hat{r})$, and the eigenvalues are $\lambda_n^{uniform} = (n(n+1)D + B)/C, n = 0, 1, \ldots, \infty$. The uniform case has been studied extensively (e.g. North and Cahalan, 1981).

The temperature departure $\tilde{T}(\hat{r},t)$ can be expanded into the non-orthogonal basis set $\psi_n(\hat{r})$ as

$$\tilde{T}(\hat{r},t) = \sum_n a_n(t)\psi_n(\hat{r}), \tag{5}$$

with

$$a_n(t) = (\psi_n, C\tilde{T}). \tag{6}$$

By inserting (5) back into (2), we can get the Fluctuation–Dissipation Equation of the Earth-Atmosphere system as

$$\dot{a}_n + \lambda_n a_n = (\psi_n, \tilde{F}) \tag{7}$$

Discussions on Fluctuation–Dissipation in climate and climate modelling can be found in Leith (1975); Hasselmann (1976); Bell (1980); North et al. (1993) and Von Storch (2004), etc. A more detailed explanation is to follow in Section 3.2.

Equation (7) represents a set of *dynamically* uncoupled equations. If $\tilde{F}(\hat{r},t)$ is suddenly set to zero, each mode amplitude, $a_n(t)$, will decay exponentially to zero with time constant $\tau_n = \lambda_n^{-1}$. Note that the driving term, $(\psi_n, \tilde{F})$ on the RHS of (7) does not include the weight function $C(\hat{r})$. So the quantities $(\psi_n, \tilde{F})$ may be statistically correlated from one mode to another even if

forcing $\tilde{F}(\hat{r}, t)$ is spatial white noise. Hence, while the members of the LHS of the system (7) are uncoupled, the RHS may have a statistical coupling: the $a_n(t)$ may then be correlated, and they are not ordinarily statistically independent. The modes will have exponentially decaying autocorrelation functions if $\tilde{F}(\hat{r}, t)$ is white noise in time, no matter what its spatial dependence is (e.g. its amplitude might be modulated by a peak in mid-latitudes, or it might be statistically rotationally invariant over the sphere, or its spatial characteristics – e.g. spatial autocorrelation functions – might be dependent on position). A more detailed explanation is to follow in section 3.2.

Another special case is assuming $C_{\text{ocean}} \to \infty$. In this case the only temperature response occurs over land for time dependent forcing and the land eigenfunctions become orthogonal (without the need for the weight function $C(\hat{r})$). At high frequencies ($f \gg 1$/year), this can be a good approximation.

2.1. A related orthogonal set

An orthogonal set can be constructed from the $\psi_n(\hat{r})$, namely,

$$\phi_n(\hat{r}) = \sqrt{C(\hat{r})}\psi_n(\hat{r}), \tag{8}$$

such that

$$(\phi_m, \phi_n) = \delta_{m,n}, \sum_n \phi_n(\hat{r})\phi_n^*(\hat{r}') = \delta(\hat{r} - \hat{r}'). \tag{9}$$

The second part of (9) is the completeness relation for the $\phi_n(\hat{r})$ (its derivation shown in Appendix), which also leads to a completeness relation for the $\psi_n(\hat{r})$:

$$\sum_n \psi_n(\hat{r})\psi_n^*(\hat{r}') = \frac{\delta(\hat{r} - \hat{r}')}{C(\hat{r})}. \tag{10}$$

While the $\phi_n(\hat{r})$ set do not satisfy a system of dynamically uncoupled equations, such as (7). However, their orthogonality tempts us to consider a possible connection to the Empirical Orthogonal Functions (EOFs). Unfortunately this does not turn out to be straightforward. Recall that there are infinitely many orthogonal basis sets in this space and this is merely one of them and the EOFs are another. The two sets are of course related by a rigid rotation (unitary transformation) but finding that transformation does not appear to be easy.

3. Response to periodic forcing

Suppose the forcing function $\tilde{F}(\hat{r}, t)$ is sinusoidal in time such that it can be represented as the real part of

$$\tilde{F}(\hat{r}, t) = F_\omega(\hat{r})e^{-i\omega t}, \tag{11}$$

Then (7) becomes

$$a_{\omega,n} = \frac{(\psi_n, F_\omega)}{\lambda_n - i\omega}, \tag{12}$$

where $a_{\omega,n} = a_n(t)e^{i\omega t}$. If $\tilde{F}(\hat{r}, t)$ is any periodic function of t it can be decomposed into a Fourier Series and the individual frequency components can be solved for independently. The example of the seasonal cycle follows.

3.1. Seasonal cycle forcing

In this case, a very good approximation to the forcing is

$$S(\mu, t) = 1 + S_{11}\cos(2\pi t)P_1(\mu) + (S_{20} + S_{22}\cos(4\pi t))P_2(\mu), \tag{13}$$

where μ is the sine of latitude (cosine of polar angle), and the time t is in units of years (North and Coakley, 1979). To obtain the response to the seasonal cycle, one simply finds the response to the three separate (angular) frequencies, $\omega = 0, 2\pi, 4\pi$, then recomposes the temperature field from the three Fourier Series components (essentially as done in NMS83).

3.2. Stationary noise forcing

Suppose $\tilde{F}(\hat{r}, t)$ is a stationary random function of time. Then the different frequency components will be uncorrelated

$$\left\langle F_\omega^*(\hat{r})F_{\omega'}(\hat{r}')\right\rangle = K_{F,\omega}(\hat{r}, \hat{r}')\delta(\omega - \omega'), \tag{14}$$

where the angular brackets denote ensemble averaging, and $K_{F,\omega}(\hat{r}, \hat{r}')$ is a covariance function of $\tilde{F}$ between points $\hat{r}$ and $\hat{r}\prime$ at angular frequency ω. Incidentally, the EOFs of $\tilde{F}$ at angular frequency ω are just the eigenfunctions of the kernel $K_{F,\omega}(\hat{r}, \hat{r}')$. This serves as a reminder that EOFs of stationary time series form a separate set for each frequency (band).

In this case, the $a_n(t)$ will also be stationary random functions of time. For an individual mode n we can write

$$\begin{aligned}\left\langle a_{\omega,n}^* a_{\omega',n}\right\rangle &= \frac{\langle (F_\omega, \psi_n)(\psi_n, F_{\omega'})\rangle}{\lambda_n^2 + \omega^2} \\ &= \frac{\iint \Psi_n^*(\hat{r})K_{F,\omega}(\hat{r}, \hat{r}')\Psi_n(\hat{r}')d\hat{r}d\hat{r}'}{\lambda_n^2 + \omega^2}\delta(\omega - \omega').\end{aligned} \tag{15}$$

If $\tilde{F}(\hat{r}, t)$ is white in time (this means $K_{F,\omega}$ is independent of ω), then each mode $a_n(t)$ behaves as a pure AR1 red noise time-series with a Lorentz power spectrum. Each mode will have an autocorrelation function that is pure exponential with decay time $\tau_n = \lambda_n^{-1}$ (Detailed derivation can also be seen in Appendix C of Wu, 2005). The individual TDM are not statistically independent of one another since the forcing components are not. By repeating the steps forming the eq. (15) for a_n and a_m, it can be shown that even if $K_{F,\omega}(\hat{r}, \hat{r}')$ is diagonal (white noise in space for the forcing) the modes a_n and a_m ($n \neq m$) will be correlated. In the next section we will draw special attention to the possibility of white noise forcing in the real world case. In the limit of $C_{\text{ocean}} \to \infty$, and in the case of white temporal noise forcing, the mode amplitudes do become statistically independent and equivalent to the EOFs.

4. Examples of TDM shapes

We construct a 64 (longitude) × 31 (sin(latitude)) plus 2 polar points on the sphere to calculate our TDMs. So there are total 1986 grid points with 1281 ocean grid points and 705 land points. The North Pole is ocean grid and the South Pole is land grid. The grids are equally spaced on this rectangular map in longitude versus sine of latitude. The mode pattern and corresponding decay time scale can be modelled through (3). Detailed numerical procedures can be found in Appendix B of Wu (2005). We obtain a total of 1281 ocean modes (corresponding to 1281 ocean grid points) and 705 land modes (corresponding to 705 land grid points).

The modes $\psi_n(\hat{r})$ are attractive for among other reasons they need only be solved for once. All time-dependent linear problems can then be expressed in terms of them. The essential difference between these modes and the EOF modes (Kim and North, 1993) is that they are spatial physical modes and their shapes do not depend on frequency as the statistical (EOF) modes do. Also, they are not strictly orthogonal like EOFs ($C(\hat{r})$ is the required weight function). This leads to their being correlated to each other.

Before describing the details of our choices of model parameters (different from, e.g. NMS83), we call attention to the TDM family-style geographic patterns. The TDMs are sorted by their decay times, the longest decay time having the lowest index. Figure 1 shows the first four TDMs which are predominantly associated with the ocean. After $n = 1282$, the modes are predominantly associated with the land masses. Figure 2 illustrates this by showing modes 1282, 1283, 1286 and 1287. This family of modes is clearly a sequence with shorter and shorter decay times and clearly associated with the land masses of Asia–Europe–Africa. The mode amplitudes over the rest of the world are negligible. These amplitudes over the oceans tend to zero in the limit $C_{\text{ocean}} \to \infty$. Figure 3 shows a similar sequence for North America. The other land masses, such as Australia, South America and Antarctica show similar families of modes that are close to zero outside their coastlines. It is worth mentioning that the TDM shapes are hardly changed when we choose different sets of parameters such as those taken from NMS83 versus from Hyde et al. 1990. The various choices of parameters $D(\hat{r})$ and B also have almost no effect on the TDM patterns. However, the changes of the eigenvalues are significant as these parameters are varied. Therefore, the TDM patterns are fairly robust with respect to a wide range of parameter choices, but their decay timescales are more sensitive to the model parameter settings.

By the linear superposition principle we can study the response of periodic or noise forcing one continent at a time. If we use the low values of sea-ice $C(\hat{r})$ over the Arctic Ocean, we find the modes for North America and Asia joined by a kind of land bridge effect (not shown).

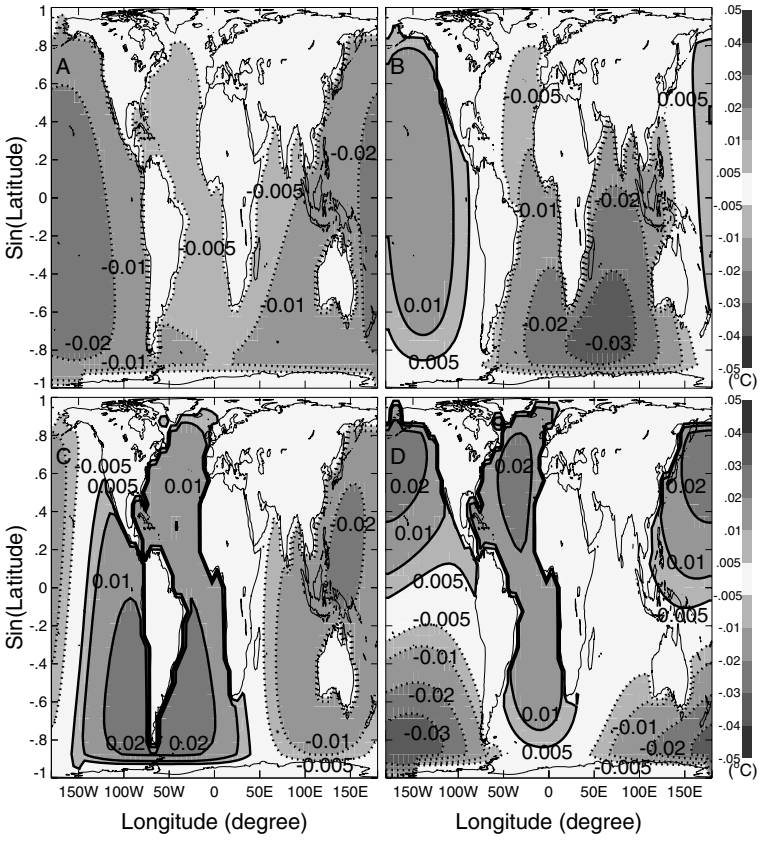

Fig. 1. Four TDMs identified with large-scale oceanic modes: (A) Mode No.1 with decay time $\tau = 0.763$ yr; (B) Mode No.2 with decay time $\tau = 0.749$ yr; (C) Mode No.3 with decay time $\tau = 0.746$ yr; (D) Mode No.4 with decay time $\tau = 0.735$ yr. The mode amplitudes over the rest of the world are negligible. The oceanic mode amplitudes are predominantly associated with the oceans.

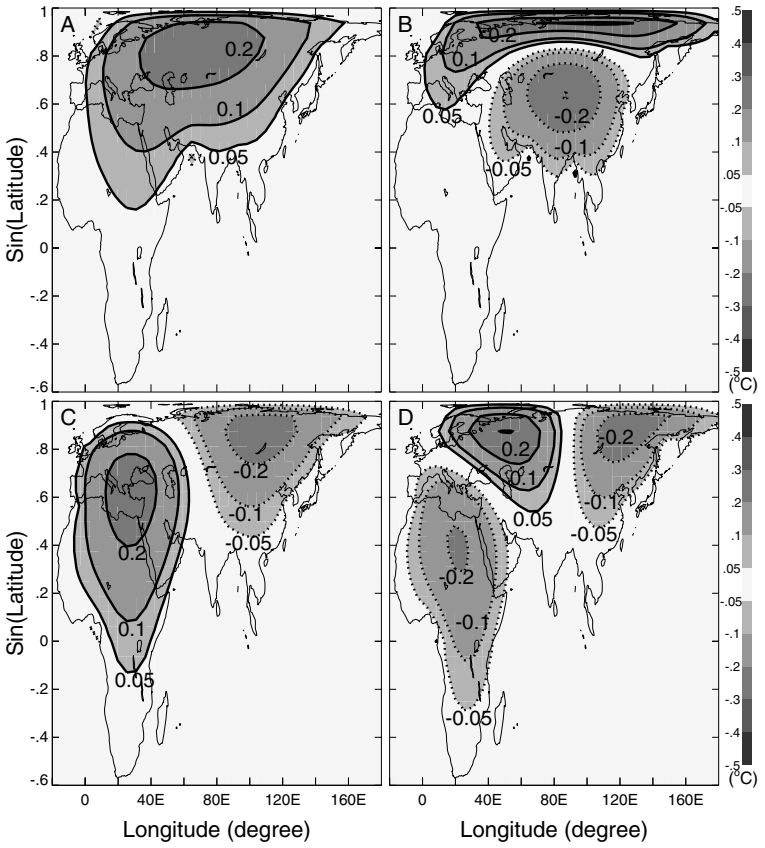

Fig. 2. Examples of Eurasian–African family modes: (A) Mode No.1282 with decay time $\tau = 0.03277$ yr; (B) Mode No.1287 with decay time $\tau = 0.01561$ yr; (C) Mode No.1283 with decay time $\tau = 0.02329$ yr; (D) Mode No.1286 with decay time $\tau = 0.01642$ yr. The mode amplitudes over the rest of the world are close to zero. The land mode amplitudes are predominantly associated with the land masses.

Figure 4 shows three (log–log) spectra of decay times $\tau_n = \lambda_n^{-1}$ as a function of mode index n. The dashed line is the spectrum of (log) the theoretical mode decay times by using the parameters in Hyde et al. (1990). This curve is strongly sloped downwards as a function of $\log n$. The dotted line is the spectrum of the estimated autocorrelation timescale of the mode amplitude time-series produced from data projection. Over land we take 20-yr (1983–2002) of near-surface air temperatures obtained from the National Centers for Environmental Prediction (NCEP) daily reanalyzed data (http://www.cdc.noaa.gov). This daily air temperature dataset is not appropriate for ocean-mode analysis because it is not able to represent the mean temperature of the ocean mixed layer. So we chose the 21-yr (1981–2001) NCEP reanalyzed weekly averaged surface temperature data for the autocorrelation analysis of ocean modes, since the ocean data are complete for this period. The weekly data are not able to be used for the analysis of land modes which have decay timescales of a few days. The data represent an average temperature from 5 to 10 m depth over ocean. We removed the trends and the seasonal cycle first and then did the projections onto each mode pattern to obtain the time-series of mode amplitude $a_n(t_k)$, $t_k = 1, 2, 3, \ldots\ldots$. Then we calculated the autocorrelation functions of $a_n(t_k)$ yielding an estimate of the autocorrelation timescales τ_n. This dotted curve is naturally noisy for several reasons. For one, the theoretical eigenvalues are very nearly the same making identification of a particular eigenfunction difficult (when eigenvalues are degenerate, linear combinations of eigenfunctions are also eigenfunctions, sometimes called 'mixing'). This ambiguity in labelling leads to a naturally noisy spectrum of empirical decay times. Another is the finite differencing scheme we employed. We used an equally spaced grid in the μ- longitude plane. The exact placement of the continents on this grid leads to a small ambiguity in the eigenvalues and eigenfunctions – these errors are sometimes evident on close examination of the maps, but not thought to be significant in our main conclusions.

One feature stands out: The spectrum of decay times is approximately flat over the modes from 1 to 1281 by data projection. This flatness indicates that the ocean modes are statistically independent of one another and therefore they are close to white noise in space. Reducing oceanic thermal diffusivity (i.e. shortening spatial correlation) is necessary in order to flatten the theoretical spectrum of mode amplitudes to match the spectrum by observations. For this reason, we adjusted the parameters over ocean to make the length scale of the oceans in the model much shorter than in earlier studies. The local diffusive length scale can be expressed as $l(\hat{r}) = \sqrt{\frac{D(\hat{r})}{B(\hat{r})}}$ and can be either reduced by lowering $D(\hat{r})$ or by increasing $B(\hat{r})$. Both actions make sense in physics because the Rossby Radius $Ro(\hat{r}) = \frac{\sqrt{g'(\hat{r}) * H(\hat{r})}}{f}$ ($g'(\hat{r})$ is a reduced acceleration due to gravity, $H(\hat{r})$ is a layer thickness, f is the Coriolis parameter) (Gill 1982) is about a factor

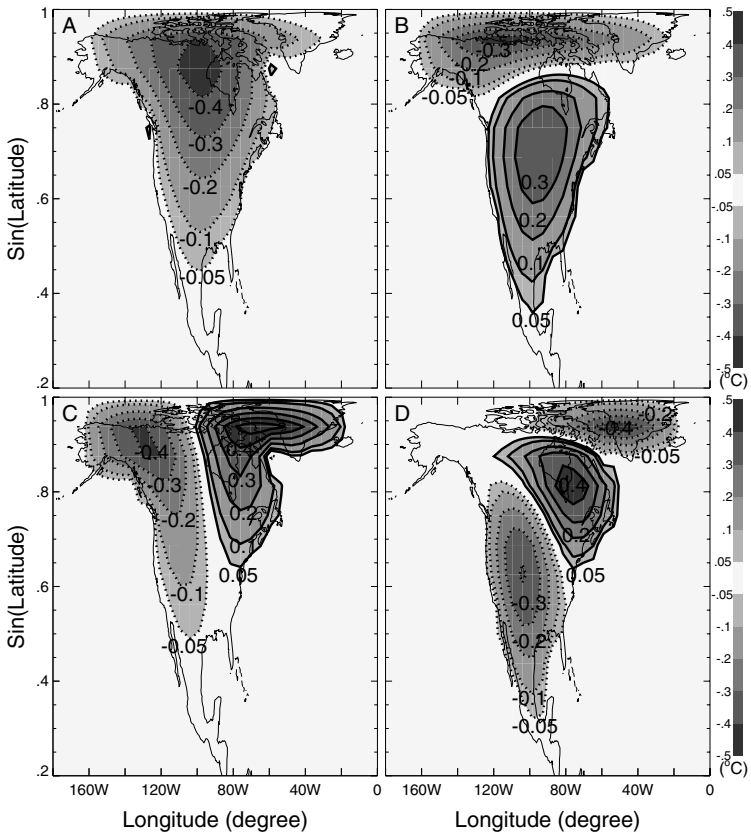

Fig. 3. Examples of North American family modes: (A) Mode No.1284 with decay time $\tau = 0.02031$ yr; (B) Mode No.1289 with decay time $\tau = 0.01191$ yr; (C) Mode No.1294 with decay time $\tau = 0.00952$ yr; (D) Mode No.1301 with decay time $\tau = 0.00747$ yr. The mode amplitudes over the rest of the world are close to zero. The land mode amplitudes are predominantly associated with the land masses.

of 10 lower over the oceans than in the atmosphere considering in the mid latitude, moreover B(ocean) should be increased to take into account the heat leakage to/from the ocean mixed layer to layers below. The theoretical decay timescales from the tuned model can capture the basic properties of the modal autocorrelation timescales from data projections even though they do not match perfectly. The flat spectrum of the estimated autocorrelation timescales over land modes is due to the resolution of the daily data. This makes the shorter timescales (less than 1 d) irresolvable. Flattening the spectrum of decay times for the ocean family of modes is a constraint not used before in EBCM tuning.

As a consistency check, we used the parameters in present tuned model (Table 1) and in previous studies (e.g. NMS83; Hyde et al. 1990) to solve the seasonal cycle using the TDMs as a basis set. The reconstructions involving only the angular frequencies $\omega = 0, 2\pi, 4\pi$ were identical to those of the earlier simulations. For completeness, we include a comparison of the annual sinusoidal response to the forcing of the seasonal cycle in Fig. 5 by using parameter values for this present study (Table 1).

Next, we wish to show the shapes of autocorrelation functions of time-series generated from the data projected onto the TDMs. The first three modes have autocorrelation functions as depicted in Fig. 6(a). The decay timescales (in Fig. 4) of the first three ocean modes are about 40, 39, 39 weeks theoretically, while about 27, 21, 19 weeks by ocean surface temperature data projection. This difference is not hard to understand considering that the real surface temperature is controlled by vertical heat transport from below the mixed layer which is not included in this version of the EBCM. Figure 6(b) shows semilog plots of the autocorrelation functions of near-surface air temperature data projected onto modes 1282, 1283 and 1284, which are the longest lived land modes. The decay timescales (in Fig. 4) by data projection are about 8, 7, 6 d which are very close to the theoretical decay timescales 12, 9, 7 d. Even though the timescales by data projection are not exactly equal to the theoretical ones for both ocean and land modes, they are all not far beyond the range of the theory. In addition, all of the curves in these figures are reasonably exponential in their appearance. This suggests that the representation in eq. (7) holds with the temporal dependence of the RHS as white noise, independent of its spatial distribution or any other properties.

A random check of other modal autocorrelation functions shows similar behaviour with the exception of a few which exhibit damped oscillatory decays. These latter are probably the result of seasonal cycle contamination and/or sampling error.

5. Conclusions

This paper has introduced a non-orthogonal set of spatial physical modes which can be used as a basis set for all subsequent

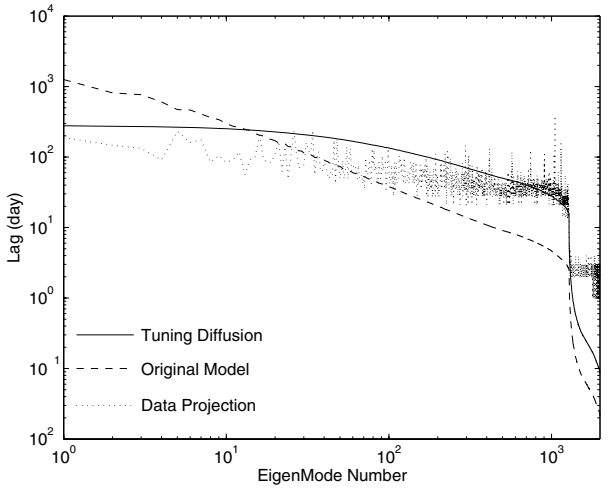

Fig. 4. Log–log spectra of decay timescales as function of mode index n. The dashed line is the spectrum of theoretical decay timescales calculated by using the parameters in Hyde et al. (1990) ('Original Model' indicates using the parameter values in the old EBCM model). The dotted line is the spectrum of the estimated autocorrelation timescales calculated by data projection onto the TDMs. The solid line is the spectrum of theoretical decay timescales from the tuned model (model parameters in this paper) with much shorter length scales over the oceans.

Table 1. Table of values of parameters used in this paper. The horizontal thermal diffusion coefficient depends on latitude through $D(\mu) = D_0(1 + D_2\mu^2 + D_4\mu^4)$ (North et al., 1983) and the co-albedo is $1 - \alpha\ (\mu) = a_0 + a_2 P_2(\mu)$, where $\mu = \sin$ (*Latitude*)(North and Coakley, 1979)

A	184.0 W m^{-2}
B^{land}	2.094 W m^{-2} K^{-1}
B^{ocean}	$2\times B^{\text{land}}$
D_0^{land}	0.505 W K^{-1}
D_0^{ocean}	$D_0^{\text{land}}/10$
D_2	-1.33
D_4	0.67
a_0	0.62
a_2	-0.20
C^{land}	0.1605 W m^{-2} K^{-1} yr
C^{ocean}	3.23 W m^{-2} K^{-1} yr
S_1	-0.796
S_2	-0.477
S_{22}	0.147
Q	340 W m^{-2}

problems for the EBCM. The modes form a complete set of temperature patterns on the globe. Those modes which are predominantly non-zero over the oceans have relatively long decay timescales (a few months to ∼1yr), while those predominantly non-zero over land have distinctly shorter ones (∼ a few days). The decay timescales are important indexes which indicate how long the thermal energy dissipation will take in surface temperature fluctuations. Mode amplitude satisfies statistically exponential decay law, that is, if forcing is abruptly halted, the mode amplitude decays exponentially. These modes in principle need only be solved once for all time-dependent linear problems. The mode amplitudes show dynamically uncoupled but statistically cross-correlated property. When temporally white noise forcing (independent of its spatial dependence of variance or point-to-point covariance) is applied in the model, the autocorrelation functions for the mode amplitudes will be exponentially decaying with lag.

The modes are proven useful in reconstructing seasonal temperature variations and in examining climate responses to noise forcing. The comparable timescales of autocorrelation of modal amplitudes with data projection of mode's decay timescale is comforting. It implies that these decay modes may be a useful complete basis set related to surface temperature fluctuations. The exponential decay pattern of the mode's autocorrelation functions produced by data projection and their similarity to the decay slopes of the theoretical ones provide a kind of support for the existence of these modes in nature.

Our experimentation with data projected onto the modes indicates that this is approximately true for data collected from the real world. This is to be expected from linear multivariate systems which obey the Fluctuation Dissipation Theorem. Previous work appears to have relied on finding steadily oscillating solutions directly. However, the development of the TDM theory makes it possible to analyse more generally time-dependent surface-temperature problems in a framework with physical interpretation. Its applications need further investigations. It could be used to examine models' abilities in simulating their thermal fluctuation decay behaviour through projecting Atmosphere-Ocean General Circulation Models surface temperature output onto these modes. In this paper, we only investigated the ocean surface temperature for ocean modes. However, it could also be used for the study of vertical ocean heat transport by coupling a 2-D EBCM system with vertical heat flux and a vertical ocean advection–diffusion model (e.g. Kim and North, 1992). Exploration of climate sensitivity (e.g. Cionni et al., 2004) by using the TDM theory is another possible avenue to be investigated.

Clearly, the TDM theory has its limitations. The fundamental assumptions of the EBCM model which are constant parameters over land and ocean (e.g. 25 m mixed-layer depth) are far away from the reality. Because of that, results by the TDM theory only provide a very rough and restricted view of the full system response. However, because of its simplicity, it is useful as a test bed for investigating and comparing with more sophisticated theories.

6. Appendix: Some mathematical terms and definitions

This appendix will refresh the reader with some notation and elementary properties of linear analysis as it applies to the present

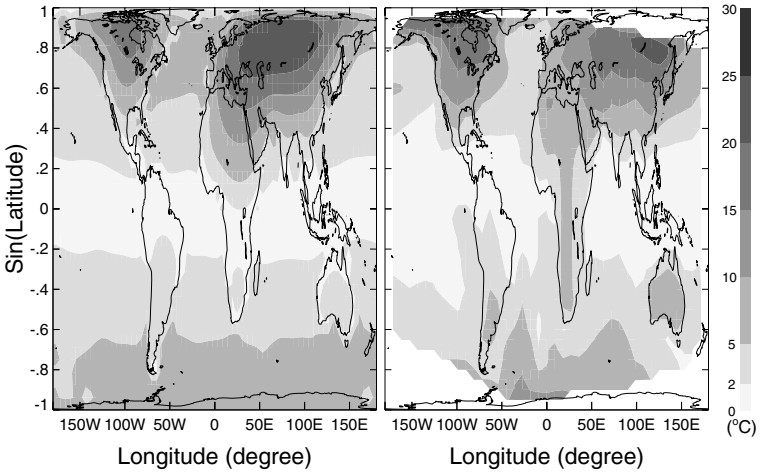

Fig. 5. The amplitude of the temperature response to annual-cycle forcing based on the linear model (left panel) and derived from the monthly temperature observations (Jones dataset at *http://www.cru.uea.ac.uk/cru/data/*, 1978–2002 data are used for the analysis) (right panel). Larger response occurs over Northern-Hemisphere continents. The temperature reaches the maximum ($\sim 25\ ^\circ$C) over central Eurasia. The model parameters are from the present paper. Note that the map projection used here is different from that in the earlier papers. Here we use as the North–South coordinate the sine of latitude.

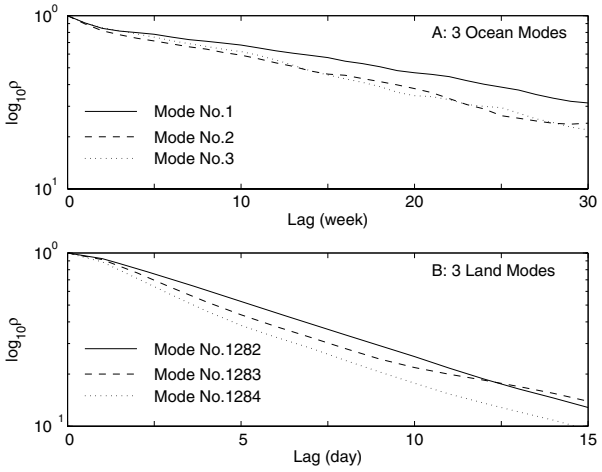

Fig. 6. Semilog plots of the autocorrelation functions for the first three data-projected modes (A): those shown in Fig. 1) and for the longest lived land modes (B): as shown in Figs 2 and 3). A straight line decay indicates exponential decay.

problem. First, consider two complex functions defined on the sphere, $\psi(\hat{r})$ and $\phi(\hat{r})$. We define the inner product as

$$(\psi, \phi) = \int \psi^*(\hat{r})\phi(\hat{r})\, d\hat{r}, \tag{16}$$

where the superscript asterisk indicates complex conjugation, and $d\hat{r}$ indicates integration with respect to solid angle over the entire sphere. If the integral vanishes, the two functions are said to be orthogonal.

7.1. Operators

Let H_1 be an operator (e.g. $-\nabla \cdot D(\hat{r})\nabla + \mathrm{B}$). If an operator has the property that

$$(\psi, H_1\phi) = (H_1\psi, \phi) \tag{17}$$

for arbitrary $\psi(\hat{r})$ and $\phi(\hat{r})$ then the operator is said to be Hermitian (e.g. $-\nabla \cdot D(\hat{r})\nabla + \mathrm{B}$ is Hermitian, which can be proven by integration by parts twice).

7.2. Eigenvalues & eigenfunctions

An eigenvalue problem posed on the sphere is of the form:

$$H_1\chi_n = \lambda_n\chi_n \tag{18}$$

where the $\chi_n(\hat{r})$ are referred to as eigenfunctions with index n, and to each corresponds an eigenvalue λ_n. If H_1 is Hermitian, it can be shown that the eigenvalues are real and that they form a discrete set with a lower bound. This means the index n can be arranged to run from 0 to ∞ over the positive integers. Furthermore, the eigenfunctions will be orthogonal, and they can be normalized such that:

$$(\chi_m, \chi_n) = \delta_{m,n}. \tag{19}$$

The eigenfunctions for *a complete set*, which means that any reasonable function defined on the sphere, can be expanded into these functions,

$$F(\hat{r}) = \sum_{n=0}^{\infty} a_n\chi_n(\hat{r}), \tag{20}$$

with

$$a_n = (\chi_n, F). \tag{21}$$

7.3. Completeness relation of orthogonal eigenfunctions

The completeness relation of orthogonal eigenfunctions $\chi_n(\hat{r})$ is

$$\sum_{n=0}^{\infty} \chi_n(\hat{r})\chi_n^*(\hat{r}') = \delta(\hat{r} - \hat{r}'). \tag{22}$$

Its derivation is as follows (by using (20), (21), (16))

$$F(\hat{r}) = \sum_{n=0}^{\infty} a_n \chi_n(\hat{r}) = \sum_{n=0}^{\infty} (\chi_n, F)\chi_n(\hat{r})$$
$$= \sum_{n=0}^{\infty} \left[\int \chi_n^*(\hat{r}')F(\hat{r}')d\hat{r}' \right] \chi_n(\hat{r})$$
$$= \int \left[\sum_{n=0}^{\infty} \chi_n^*(\hat{r}')\chi_n(\hat{r}) \right] F(\hat{r}')\, d\hat{r}'$$

7.4. Non-orthogonal eigenfunctions

In this paper we need to address a slight generalization of the above,

$$H_1\psi_n = \lambda_n H_2 \psi_n, \tag{23}$$

where both H_1 and H_2 are Hermitian. The following properties are easily proven by very straightforward techniques (detailed seen Appendix A of Wu (2005)):

1. The λ_n are real; $n = 0, \ldots, \infty$.
2. Orthogonality with weight function $(\psi_m, H_2\psi_n) = \delta_{m,n}$

These definitions and properties should be enough for most readers of this paper, but they are a mere refresher. For a more complete discussion readers are referred to the mathematical physics literature.

8. Acknowledgments

It is a pleasure to thank Mr. and Mrs. Harold J. Haynes whose endowment to Texas A&M University helped to support this project. Early parts of the work were supported by a grant from the Global Change Program of the National Oceanic and Atmospheric Administration. We thank Professors Ping Chang and Robert Dickinson for helpful discussions. We also thank two reviewers for constructive comments.

References

Bell, T. L. 1980. Climate sensitivity from fluctuation dissipation: some simple model tests. *J. Atmos. Sci.* **37**, 1700–1707.

Cionni, I., Visconti, G. and Sassi, F. 2004. Fluctuation dissipation theorem in a general circulation model. *Geophys. Res. Lett.* **31**, L09206, doi: 10.1029/2004GL019739.

Frame, D. J., Booth, B. B. B., Kettleborough, J. A., Stainforth, D. A., Gregory, J. M., Collins, M. and Allen, M. R. 2005. Constraining climate forecasts: The role of prior assumptions. *Geophys. Res. Lett.* **32**, L09702, doi: 10.1029/2004GL022241.

Gill, A. E. 1982. *Atmosphere-Ocean Dynamics*. Academic Press, 662 pp.

Graves, C. E., Lee, W.-H. and North, G. R. 1993. New parametrizations and sensitivities for simple climate models. *J. Geophys. Res.* **98**, 5025–5036.

Hasselmann, K. 1976. Stochastic climate models. Part I: Theory. *Tellus* **28**, 473–484.

Hegerl, G. C., Crowley, T. J., Hyde, W. T. and Frame, D. J. 2006. Climate sensitivity constrained by temperature reconstructions over the past seven centuries. *Nature* **440**, 1029–1032.

Horn, R. A. and Johnson, C. R. 1985. *Matrix Analysis*. Cambridge University press, 561 pp.

Hyde, W. T., Kim, K.-Y., Crowley, T. J. and North, G. R. 1990. On the relation between polar continentality & climate: studies with a nonlinear seasonal energy balance model. *J. Geophys Res.* **95**, 18653–18668.

Kim, K.-Y. and North, G. R. 1992. Seasonal cycle and second-moment statistics of a simple coupled climate system. *J. Geophys. Res.* **97**, 20437–20448.

Kim, K.-Y. and North, G. R. 1993. EOF analysis of surface temperature field in a stochastic climate model. *J. Climate* **6**, 1681–1690.

Leith, C. E. 1975. Climate response and fluctuation dissipation. *J. Atmos. Sci.* **32**, 2022–2026.

Lindzen, R. S. and Farrell, B. 1977. Some realistic modifications of simple climate models. *J. Atmos. Sci.* **34**, 1487–1501.

North, G. R. and Coakley, J. A. 1979. Differences between seasonal and mean annual energy balance model calculations of climate and climate change. *J. Atmos. Sci.* **36**, 1189–1204.

North, G. R. and Cahalan, R. F. 1981. Predictability in a solvable stochastic climate model. *J. Atmos. Sci.* **38**, 504–513.

North, G. R., Cahalan, R. F. and Coakley, J. A. 1981. Energy balance climate models. *Rev. Geophys. Sp. Phys.* **19**, 91–121.

North, G. R., Mengel, J. G. and Short, D. A. 1983. A simple energy balance model resolving the seasons and the continents: Application to the Milankovitch theory of the ice ages. *J. Geophys. Res.* **88**, 6576–6586.

North, G. R., Bell, R. E. and Hardin, J. W. 1993. Fluctuation dissipation in a general circulation model. *Clim. Dyn.* **8**, 259–264.

Stevens, M. J. and North, G. R. 1996. Detection of the climate response to the solar cycle. *J. Atmos. Sci.* **53**, 2594–2608.

Von Storch, J.-S. 2004. On statistical dissipation in GCM-climate. *Clim. Dyn.* **23**, 1–15.

Wu, W. 2005. Linear analysis of surface temperature dynamics and climate sensitivity. *Dissertation*. Texas A&M University, College Station, USA, pp. 81.